Applied Mathematics and Computation 469 (2024) 128528

Contents lists available at ScienceDirect

Applied Mathematics and Computation

journal homepage: www.elsevier.com/locate/amc

Full Length Article

High-order well-balanced numerical schemes for one-dimensional shallow-water systems with Coriolis terms

Víctor González Tabernero [a,*], Manuel J. Castro [b], J.A. García-Rodríguez [a]

[a] Departamento de Matemáticas, Facultad de Informática and CITIC, Campus Elviña s/n, A Coruña (Spain), 15071, A Coruña, Spain
[b] Departamento de Análisis Matemático, Facultad de Ciencias, University of Málaga, Campus de Teatinos s/n, Málaga, 29080, Spain

A B S T R A C T

The goal of this work is to develop high-order well-balanced schemes for the one-dimensional shallow-water equations with Coriolis terms. The main contribution is the development of general numerical methods that allow the achievement of arbitrary high-order for the shallow-water equations with Coriolis terms while preserving all the stationary solutions.

1. Introduction

The goal of this work is to develop high-order well-balanced schemes for the one-dimensional shallow-water equations with Coriolis terms. The main novelty of this article is the development of general numerical methods that allow to capture all stationary solutions of the shallow-water equations with Coriolis terms, with arbitrary high-order accuracy. To the best of our knowledge, this is the first time in the literature, that such a general technique is presented for the construction of high-order well-balanced numerical methods in the context of 1D shallow-water equations with Coriolis forces.

This problem fits into the more general framework of building high-order schemes for balance laws

$$\partial_t U + \partial_x f(U) = s(x,U), \qquad U \in \mathbb{R}\times\mathbb{R}^+ \to \Omega \subset \mathbb{R}^N, \quad f \in C^1(\mathbb{R}^N,\mathbb{R}^N), \quad s:\ \mathbb{R}\times\Omega \mapsto \mathbb{R}^N, \tag{1}$$

that are well-balanced. That is numerical schemes that preserve, in a sense that will be detailed later, all or certain families of stationary solutions of the system.

The construction of well-balanced schemes is a very challenging task that has been of great interest in research during the last decades, giving rise to a large number of publications on the subject and continues to be a very active field of research.

One of the first papers that focused on developing numerical schemes that were able to preserve stationary solutions was [5]. There the authors introduced a new numerical concept called the C-Property (*conservation property*) for the balance law given by a shallow-water system of equations.

This property consisted in endowing the numerical scheme with the capability to preserve one particular stationary solution: water at rest, that is, preserving the flat free surface of the fluid in the absence of movement. The idea of C-Property can be extended to any balance law with steady-state solutions. In a more general scenario, this property is related to the capacity of a numerical scheme to preserve the stationary solutions of the system of balance laws. Since that seminal paper, many works can be found in the literature about defining well-balanced schemes for balance laws, for different models, for example:

* Corresponding author.
E-mail addresses: v.gonzalez.tabernero@udc.es (V. González Tabernero), mjcastro@uma.es (M.J. Castro), jose.garcia.rodriguez@udc.es (J.A. García-Rodríguez).

https://doi.org/10.1016/j.amc.2023.128528
Received 20 March 2023; Received in revised form 24 October 2023; Accepted 31 December 2023

Available online 12 January 2024

in the context of shallow-water and water-at-rest solutions ([5], [7], [2], [6], [10], [18], [20], [21], [8], [41], [12], [11], [13], [31], and references therein); for shallow-water equations with Coriolis forces ([23], [16], [26], [9], [38], [3]); for Euler equations with gravity ([22], [28], [33]); Ripa system [34] and for multidimensional balance laws ([4]) or [15] for a review on the subject.

In this work, we follow the general framework proposed by [14] to define well-balanced numerical schemes for balance laws. We start by considering a general semi-discrete high-order FV scheme for (1). The computational domain is split into FV cells, $I_i = \left[x_{i-\frac{1}{2}}, x_{i+\frac{1}{2}}\right]$, with constant size $|I_i| = \Delta x$. $U_i(t)$ is the averaged solution in the i-th volume at time t

$$U_i(t) \cong \frac{1}{|I_i|} \int_{x_{i-\frac{1}{2}}}^{x_{i+\frac{1}{2}}} U(x,t)\, dx.$$

With this notation, the FV scheme can be written as:

$$\frac{dU_i}{dt} = -\frac{1}{|I_i|}\left(F_{i+\frac{1}{2}}(t) - F_{i-\frac{1}{2}}(t)\right) + \frac{1}{\Delta x} S_i, \tag{2}$$

where $F_{i+\frac{1}{2}} = \mathbb{F}(U^{t,-}_{i+\frac{1}{2}}, U^{t,+}_{i+\frac{1}{2}})$, where $\mathbb{F}$ is a consistent numerical flux. $U^{t,\pm}_{i+\frac{1}{2}}$ are the reconstructed values at the volume edges,

$$U^{t,-}_{i+\frac{1}{2}} = P^t_i(x_{i+\frac{1}{2}}), \quad U^{t,+}_{i+\frac{1}{2}} = P^t_{i+1}(x_{i+\frac{1}{2}}),$$

being $P^t_i(x)$ a reconstruction operator of order p at the volume V_i. $P^t_i(x)$ is obtained using a set of averaged values of the solution in the neighbour cells. This set is called the stencil and can be denoted as $(\cup_{j\in S_i} I_j)$, with S_i being the collection of the indices of neighbour volumes to I_i. With this notation, the reconstruction operators can be written as $P^t_i(x) = P_i(x; \{U_j(t)\}_{j\in S_i})$. Finally, the source integral is approximated by

$$S_i \approx \int_{x_{i-\frac{1}{2}}}^{x_{i+\frac{1}{2}}} s(x, P^t_i(x))\, dx. \tag{3}$$

Also, in the rest of the paper, we will denote by:

$$\bar{U}_i = \frac{1}{|I_i|} \int_{x_{i-1/2}}^{x_{i+1/2}} U(x)\, dx, \quad U_i \approx \bar{U}_i, \quad U_{i+1/2} \approx U(x_{i+1/2}),$$

the averages, their approximations, and the pointwise value at the cell edges, for U. Following [16], [14], a well-balanced method can be built by considering well-balanced reconstruction operators:

Definition 1.1. A reconstruction operator for U^*, P_i, related to the set of exact averages $\{\bar{U}^*_i\}$ (or their approximations $\{U^*_i\}$), is WB when

$$P_i(x) = U^*(x), \quad \forall x \in [x_{i-\frac{1}{2}}, x_{i+\frac{1}{2}}], \tag{4}$$

Finally, the following definition can be set ([29])

Definition 1.2. The semi-discrete numerical scheme (2) is *exactly WB* when the sequence of the exact averages $\{\bar{U}^*_i\}$ (or their approximations $\{U^*_i\}$) of a stationary solution U^* of (1), is also a stationary solution of the ODEs system (2).

In [14] a technique to obtain well-balanced reconstruction operators from standard ones was presented. This technique will be reviewed in section 2. The critical step of this procedure is solving the following non-linear problem for each cell and time step:

$$\begin{cases} \partial_x f(U) = s(x,U), \\ \dfrac{1}{|I_i|} \displaystyle\int_{x_{i-1/2}}^{x_{i+1/2}} U(x)\, dx = U_i. \end{cases} \tag{5}$$

After solving (5) at the volume, the obtained solution, $U^*_i(x)$ is extended to the whole stencil. In certain situations, it is not possible to obtain the exact solutions of (5). In this case, $U^*(x)$ will be replaced by a suitable approximation that will be denoted by $\widetilde{U}^*(x)$.

Following [29], in this case, the semi-discrete numerical scheme (2) is well-balanced, if the sequence of cell averages computed from the approximation $\widetilde{U}^*(x)$, and denoted by $\{U_i^*\}$, is an equilibrium of the system of ODEs (2).

In this work, we will focus on the one-dimensional shallow-water system with Coriolis terms. The system is given by:

$$\partial_t U + \partial_x f(U) = s(x,U), \quad s = s^B + s^C \tag{6}$$

where

$$U = \begin{bmatrix} h \\ hu \\ hv \end{bmatrix}, \; f(U) = \begin{bmatrix} hu \\ hu^2 + \frac{1}{2}gh^2 \\ huv \end{bmatrix}$$

are the conserved variables and the flux in the x direction respectively, and

$$s^B = \begin{bmatrix} 0 \\ -gh\partial_x z \\ 0 \end{bmatrix} \quad s^C = \begin{bmatrix} 0 \\ fhv \\ -fhu \end{bmatrix}$$

are the source terms due to the bottom topography and the Coriolis forces respectively.

Several works about developing well-balanced numerical schemes for system (6) can be found in the literature. For example, in [16] the authors focused on the simulation of the geostrophic adjustment and developed 1st-order Roe schemes and some higher-order extensions, to obtain good approximations for inertial oscillations, and also studied the wave amplifications of the schemes, together with the well-balancedness properties for the steady states corresponding to $u = 0$ and $v = C$, $C \in \mathbb{R}$. In [23] the authors developed first and second-order schemes for the shallow-water equations with bottom topography and Coriolis forces that preserve the water height positivity. They used non-local potential operators to obtain a well-balanced numerical scheme up to second-order, for the steady states with $u = 0$. They also consider its natural extension to 2D problems. In [26] the problem of developing a fully well-balanced scheme for the one-dimensional shallow-water system with Coriolis terms is also addressed. This article describes a technique to obtain well-balanced second-order schemes for the system. Other interesting papers dealing with the definition of well-balanced numerical methods for the shallow-water system with Coriolis are ([9], [38], [3]).

In this work we will follow the strategy presented in [14] in combination with CWENO reconstruction operators (see [24]) to define arbitrary high-order exactly well-balanced steady states with $u \neq 0$. The special case $u = 0$ will be also discussed. The main difference between the cited papers with the present approach is that, because of the generality of our technique, it allows the building of arbitrary high-order numerical schemes, not restricted to second-order.

Also, we propose 1-dimensional schemes. For the 2-dimensional schemes, there is a first work [39] to be published where we follow an extension of the numerical scheme proposed in [23]. In this and future works we are combining local and global solvers to determine stationary solutions for the system.

The outline of this paper is as follows.

In Section 2 the general well-balanced reconstruction procedure described in [16] and [14] is summarised. In Section 3 we present the high-order well-balanced numerical schemes for the shallow-water equations with Coriolis effects, focusing on the determination of the local stationary solutions for the different reconstruction orders. In Section 4 several numerical experiments are presented to numerically assess the well-balanced and high-order properties of the presented numerical schemes. Most of the numerical examples considered here have been proposed previously in [23] and [26]. In the appendix A the general technique for building arbitrary-order well-balanced CWENO schemes is detailed, while a third-order example is presented.

2. Well-balanced reconstruction procedure

In this section we review the general method presented in [16] and [14] to design high-order well-balanced reconstruction operators. This method uses a local steady state defined in the stencil of the reconstruction operator in combination with a standard reconstruction operator applied to the cell-average fluctuations.

In what follows we will consider that the cell averages are computed by a quadrature formula

$$U_i^n = \sum_{k=0}^{M} \alpha_k^i U(x_k^i, t^n), \tag{7}$$

where α_k^i are the $M+1$ quadrature weights in cell C_i associated with the $M+1$ quadrature points $x_k^i \in [x_{i-1/2}, x_{i+1/2}]$. Notice that the order of accuracy of the quadrature formula must be equal to or greater than the order of the reconstruction operator.

Thus, following [16], and given a family of cell averages $\{U_i\}$ (we drop the time dependency for simplicity), at every cell I_i, the strategy to build a well balanced reconstruction operator P_i (in the sense of the Definition 1.1) starting from a standard operator Q_i, involves the following three steps:

1. Determine the local stationary solution U_i solving the following ODE

$$\begin{cases} f_x(U_i^*) &= s(x, U_i^*), \\ \sum_{m=0}^{M} \alpha_m^i U_i^*(x_m^i) &= U_i. \end{cases} \tag{8}$$

Determining these local stationary solutions is the most nightmarish step of this procedure. If it is not possible to find this local steady state on the stencil, we set $U_i^* \equiv 0$.

2. Calculate the *fluctuations* $\{V_j\}_{j\in S_i}$

$$V_j = U_j - \sum_{m=0}^{M} \alpha_m^j U_i^*(x_m^j), \quad j \in S_i,$$

and the reconstruction operator:

$$Q_i(x) = Q_i(x; \{V_j\}_{j\in S_i}).$$

3. Compute

$$P_i(x) = U_i^*(x) + Q_i(x). \tag{9}$$

In [14], it is proved that if Q_i is conservative, also is P_i; and both operators reach the same order p, for smooth stationary solutions. Finally, if Q_i is exact for the null function, P_i is also well-balanced.

Note that, if there is no stationary solution defined in the stencil satisfying (7), we fix $U_i^* \equiv 0$, that is, the fluctuations are null and the reconstruction procedure defaults to the standard reconstruction. This is reasonable and does not have any undesirable side effect, regarding the well-balancednes of the scheme. In that situation, the stencil's cell values cannot be averages of any equilibrium solution, and therefore there is no stationary solution that the scheme should preserve, or that can be preserved. In the opposite situation, if there exists more than one stationary solution satisfying (7), we must use a criterium depending on the physics of the problem, to select among all the possible solutions.

As pointed out in [14], the WB property of the scheme can be lost due to the numerical integration of the source term (3). Here, the authors rewrite S_i as follows

$$\begin{aligned} \int_{x_{i-\frac{1}{2}}}^{x_{i+\frac{1}{2}}} S(x, P_i^t(x))\, dx &= f\left(U_i^{t,*}(x_{i+\frac{1}{2}})\right) - f\left(U_i^{t,*}(x_{i-\frac{1}{2}})\right) \\ &\quad + \int_{x_{i-\frac{1}{2}}}^{x_{i+\frac{1}{2}}} S(x, P_i^t(x)) - S(x, U_i^{t,*}(x))\, dx, \end{aligned} \tag{10}$$

being $U_i^{t,*}$ the stationary solution computed of step one. Finally, the quadrature of S_i reads:

$$S_i = f\left(U_i^{t,*}(x_{i+\frac{1}{2}})\right) - f\left(U_i^{t,*}(x_{i-\frac{1}{2}})\right) + \Delta x \sum_{m=0}^{M} \alpha_m^i \left(S(x_m^i, P_i^t(x_m^i)) - S(x_m^i, U_i^{t,*}(x_m^i))\right). \tag{11}$$

Thus, (2) is replaced by

$$\begin{aligned} \frac{dU_i}{dt} = \frac{1}{\Delta x}\Big(& F_{i-1/2} - f(U_i^{t,*}(x_{i-1/2})) - F_{i+1/2} + f(U_i^{t,*}(x_{i+1/2})) \\ & + \sum_{m=0}^{M} \alpha_m^i \left(S(P_i^t(x_m^i)) - S(U_i^{t,*}(x_m^i))\right) dx \Big). \end{aligned} \tag{12}$$

The following theorem can be proved (see [14,29])

Theorem 2.1. *Given a well-balanced reconstruction operator, related to a stationary solution $U^*(x)$, the obtained numerical scheme (12) is exactly well-balanced attending to the Definition 1.2.*

Remark. The previous procedure could be adapted in the case in which only a particular subset of stationary solutions is to be preserved (see [14]. Moreover, the case of non-smooth steady states due to the presence of singular source terms could also be addressed following the strategy described in [14].

Remark 2.2. In the proof of Theorem 2.1, the fact that the steady states are continuous and the numerical flux is consistent plays a crucial role. In the case of non-smooth steady states, some extra hypothesis on the numerical flux must be required, to achieve the same results.

In what follows the particular form of 1st, 2nd and 3rd order schemes will be described.

Remark. Time integration is performed with an SSP Runge-Kutta method. See, for example, [30].

2.1. 1st and 2nd order schemes

For the 1st and 2nd order methods, a second-order quadrature formula is applied. Therefore, it is sufficient to use the midpoint formula, thus

$$U_i \approx \frac{1}{\Delta x}\int_{x_{i-1/2}}^{x_{i+1/2}} U(x) = u(x_i) + \mathcal{O}(\Delta x^2).$$

Therefore, all the integrals involved in the definition of the numerical scheme will be approximated by the midpoint formula. In particular, the initial condition is given by

$$U_i^0 = U_0(x_i),\ \forall i.$$

Now, given the approximation of the cell averages at time t $\{U_i^t\}$, the steps to define the well-balanced reconstruction reduce to (we drop the time dependency for simplicity):

1. Compute the local stationary solution that satisfies (8) such that
$$U_i^*(x_i) = U_i.$$
2. Calculate the fluctuations.
   (a) In the first-order reconstruction, only one fluctuation is calculated
   $$V_i = U_i - U_i^*(x_i) = 0,$$
   which is cancelled by construction.
   (b) For the second-order reconstructions, three fluctuations have to be computed
   $$V_j = U_j - U_i^*(x_j),\ j = i-1, i, i+1.$$
3. Calculate the reconstruction of the fluctuations
   (a) The trivial first-order reconstruction reduces to:
   $$Q_i^n(x; V_i) = V_i = 0.$$
   (b) For second-order reconstructions, a MUSCL reconstruction with slope σ_i^n is applied, where the reconstruction operator reads
   $$Q_i^n(x; V_{i-1}, V_i, V_{i+1}) = \sigma_i(x - x_i),$$
   because $V_i = 0$. For this case, we choose the slope to be determined with the minmod limiter. As usual, the previous definition must be understood component-wise.
4. Finally, the reconstruction operator will be
   (a) For first-order it reduces to
   $$P_i(x) = U_i^*(x).$$
   (b) For second-order:
   $$P_i(x) = U^*(x) + \sigma_i(x - x_i).$$

Finally, since we are using the midpoint rule, we have

$$\int_{x_{i-1/2}}^{x_{i+1/2}} \left(S(x, P_i(x)) - S(x, U_i^*(x))\right) dx \approx \Delta x_i \left(S(x_i, P_i(x_i)) - S(x_i, U_i^*(x_i))\right) = 0,$$

as $P_i(x_i) = U_i^*(x_i)$. Thus, the ODE system (12) reduces to

$$\frac{dU_i}{dt} = \frac{1}{\Delta x_i}\Big(F_{i-1/2} - f(U_i^*(x_{i-1/2})) - F_{i+1/2} + f(U_i^*(x_{i+1/2}))\Big), \tag{13}$$

where

$$F_{i+1/2} = \mathbb{F}(P_i(x_{i+1/2}), P_{i+1}(x_{i+1/2})).$$

Attending to the determination of the local stationary solutions, the solution only needs to be known in a small set of points. Those points are the quadrature points used to compute the integrals in every cell in the stencil, and the intercell points to evaluate the fluxes. This motivates the following definition.

Definition 2.3 *(Points of interest).* Given a (exactly) well-balanced finite volume scheme, we define points of interest of a stencil $\mathcal{S}_i$ as the set of points in the domain $x \in \Omega(\mathcal{S}_i)$ where the local stationary solution has to be evaluated.

Therefore, the points of interest are:

1. For the first-order reconstruction: these points are $\{x_{i-1/2}, x_i, x_{i+1/2}\}$.
2. For the second-order reconstruction: the points of interest are $\{x_{i-1}, x_{i-1/2}, x_i, x_{i+1/2}, x_{i+1}\}$.

2.2. Third-order scheme

The third-order scheme is defined using the CWENO3 reconstruction operator. A brief overview of the procedure to define the CWENO reconstruction operator is given in Appendix A. In the case of third-order schemes, the 2-point Gauss-Legendre quadrature is used:

$$\int_{x_{i-1/2}}^{x_{i+1/2}} U(x)dx = \Delta x \frac{U(x_i - \Delta x\frac{1}{2\sqrt{3}}) + U(x_i + \Delta x\frac{1}{2\sqrt{3}})}{2} = \Delta x \frac{u(x_i^0) + u(x_i^1)}{2}.$$

Unfortunately, for this order, we are no longer able to simplify the form of the numerical scheme and the general form (12) is used. In this case, the points of interest are

$$\{x_{i-1}^0, x_{i-1}^1, x_{i-1/2}, x_i^0, x_i^1, x_{i+1/2}, x_{i+1}^0, x_{i+1}^1\}.$$

In the next section, we describe the steady states of the shallow-water system with Coriolis forces and we describe the algorithm that we use to solve the first step of the reconstruction procedure, that is, the way the local steady states are computed from the cell averages of the solution at each time step.

3. Well-balanced schemes for the shallow-water system with Coriolis forces

In this section, we show how to apply the procedure of section 2 to build 1st, 2nd and 3rd-order schemes for the one-dimensional shallow-water equations with Coriolis terms.

Remind that the shallow-water equations, with Coriolis forces in 1d, are described by the system:

$$\begin{aligned} &\partial_t h + \partial_x(hu) = 0,\\ &\partial_t(hu) + \partial_x\left(hu^2 + \frac{gh^2}{2}\right) = fhv - gh\partial_x z,\\ &\partial_t(hv) + \partial_x(huv) = -fhu, \end{aligned} \tag{14}$$

where, h is the fluid depth, hu and hv are the horizontal moments, z is the bottom topography and g and f are the gravity and Coriolis constants, respectively.

Concerning the steady states, two families can be distinguished. The case of moving steady states, that is $u \neq 0$, and the case where $u = 0$. In the first case, the steady states are the solution of the ODE system

$$\partial_x\left(hu^*\right) = 0, \tag{15}$$

$$\partial_x\left(\frac{(u^*)^2}{2} + g(h^* + z)\right) = fv^*, \tag{16}$$

$$\partial_x v^* = -f. \tag{17}$$

Now, integrating (17) we obtain that

$$v^*(x) = -fx + v_0,$$

where v_0 is a given constant. Equation (15) implies that $(hu)^*(x) = q_0$, where q_0 is a given constant.

Finally, equation (16) could be rewritten as follows

$$\frac{(u^*)^2}{2} + g(h^* + z) - fV^* = E,$$

where E is again a given constant and V^* is a primitive of v^*, that is

$$V^*(x) = -f\frac{x^2}{2} + v_0 x + v_1,$$

where we can choose $v_1 = 0$ without losing generality. In this way, the steady states for $u \neq 0$ are described by the following set of algebraic equations

$$(hu)^* = q_0 \tag{18}$$

$$\frac{(u^*)^2}{2} + g\left(h^* + z - \frac{f}{g}V^*\right) = E \tag{19}$$

$$v^* = -fx + v_0 \tag{20}$$

$$V^* = -f\frac{x^2}{2} + v_0 x, \tag{21}$$

where q_0, E and v_0 are some given constants that characterise the steady states.

Another interesting family of steady states are those corresponding to $u = 0$. In this case, for any integrable v^*, the steady states are characterised by the following expressions

$$h^*(x) = \frac{E}{g} - z + \frac{f}{g}\int v^*(x) \tag{22}$$

$$u^* = 0. \tag{23}$$

Note that one could obtain a smooth (continuous) h^* even for non-smooth v^*.

In what follows we are going to describe the reconstruction procedure for 1st, 2nd and 3rd order schemes.

3.1. First and second-order reconstructions

Remember that the first step of the reconstruction procedure consists on determine a local steady state whose cell average coincides with the one at the given time at the intercell, that is, we must find a steady state solution of (15)-(17) such that $h_i^*(x_i) = h_i$, $(hu)_i^*(x_i) = (hu)_i$ and $(hv)_i^*(x_i) = (hv)_i$. Let us consider first the case where $u \neq 0$.

It is clear from (18) than $(hu)_i^*(x) = (hu)_i$. Next, it is simple to determine $v_i^*(x)$. Taking into account that v^* is a linear function, it is straightforward to check that $v_i^*(x) = -f(x - x_i) + v_i$, where

$$v_i = \frac{(hv)_i}{h_i}.$$

Note that v_i is still a second-order approximation of the cell average. Now, it is possible to compute $V_i^*(x)$. Integrating v_i^* we obtain that

$$V_i^*(x) = -f\frac{x^2}{2} + (fx_i + v_i)x. \tag{24}$$

Note, that with this choice, V_i^* coincides with V^* given in (21), in the case of a steady state.

Now, we could obtain the constant E_i evaluating (19) at x_i, that is

$$E_i = \frac{(u_i)^2}{2} + g\left(h_i + z(x_i) - \frac{f}{g}V_i^*(x_i)\right), \tag{25}$$

where

$$u_i = \frac{(hu)_i}{h_i}.$$

Now, with this value of E_i it is possible to compute $h_i^*(x_p)$ at each point of interest x_p solving the following cubic polynomial

$$g(h_i^*)^3(x_p) + \left(gz(x_p) - fV_i^*(x_p) - E_i\right)(h_i^*)^2(x_p) + \frac{(hu)_i^2}{2} = 0. \tag{26}$$

As in the case of the standard shallow-water system, (26) has always a negative root and may have one, two or no positive roots. Here, we follow the same procedure that the one described in [17], [13] and [19] to select the appropriate value of h^* at the given point. The general principle that we follow is to maintain the fluid regime locally. Nevertheless, some difficulties appear in the neighbourhood of a critical point, that is a point where the Froude number, $F_r = |u|/\sqrt{gh} = 1$. In this case, the behaviour is similar to the shallow-water system with $f = 0$. This means, that

a) Either (26) has no admissible solutions, which means, it has two complex solutions and one negative for h.
b) Or it has two solutions for h. One solution corresponds to the supercritical regime and the other to the subcritical regime. In this case, we are not able to choose the right regime as it is not well defined due to $Fr = 1$.

The previous procedure can be summarised in the following algorithm

1. We define $v_i = (hv)_i/h_i$. In this way, $v_i^*(x)$ can be computed in the stencil as well as V_i^* using (24).
2. $(hu)_i^*(x)$ is set by the constant value hu_i in the stencil, and we define $u_i = (hu)_i/h_i$.
3. Next, we compute the value of the energy E_i at x_i using (25), and thus we can obtain the values of h_i^* at each point of interest calculating the roots of (26) using the local information of the fluid regime according to the Froude number.
4. Once the local steady state is computed in the stencil, the fluctuations concerning that particular local steady state are computed and the standard reconstruction operator applied to the fluctuations is defined.
5. Finally the reconstruction operator is defined for each conserved variable h, hu and hv.

The previous procedure in combination with (13) defines a semi-discrete first or second-order, depending on the reconstruction operator, exactly well-balanced finite volume scheme for system (14) for $u \neq 0$ steady states, where $F_{i+1/2}$ is an arbitrary consistent flux for the homogeneous system. Finally, ODE (13) is discretized using 1st or 2nd order RK TVD schemes (see [30]).

Let us now describe the reconstruction procedure for steady states with $u = 0$. In this case, for any arbitrary v, the water depth is given by

$$h^*(x) = \frac{E}{g} - z + \frac{f}{g}V^* \tag{27}$$

where V^* is a continuous primitive of v.

Note, that in this case, the steady states depend on the functional form of any arbitrary function v, therefore we cannot expect to obtain a numerical scheme that is exactly well-balanced according to the Definition 1.2 for any arbitrary choice of v. For this reason, we propose a simple strategy to define approximate steady states that approximates the exact ones, and how the previous strategy could be applied to preserve those.

Let us start with the first-order scheme. The first step is the definition of the approximated steady states. Thus, we consider now an approximation of v given by some reconstruction operator for the physical variable v. Here we set that $P_i^v(x) = v_i = (hv)_i/h_i$ and we also consider that $v_i^*(x) = P_i^v(x) = v_i$. Next $V_i^*(x)$ is defined by

$$V_i^*(x) = v_i(x - x_i) + K_i \tag{28}$$

where K_i is a constant to be fixed such that

$$V_i^*(x_{i-1/2}) = V_{i-1}^*(x_{i-1/2}).$$

Setting $K_0 = 0$ then

$$K_i = \frac{v_i + v_{i-1}}{2}\Delta x + K_{i-1}, \quad i = 1, \cdots$$

Note that $V^*(x)$ defined as $V^*(x)_{|_{C_i}} = V_i^*(x)$ is a continuous primitive of $v^*(x)$, where $v^*(x)_{|_{C_i}} = v_i^*(x) = v_i$. Once the potential $V_i^*(x)$ is computed, then $h_i^*(x)$ is defined by

$$h_i^*(x) = \frac{E_i}{g} - z(x) + \frac{f}{g}V_i^*(x). \tag{29}$$

Finally $(hu)_i^*(x) = 0$, as $u = 0$. Thus, the approximated steady states are defined by:

$$h^*(x) = \frac{E}{g} - z(x) + \frac{f}{g}V^*(x)$$
$$u^* = 0,$$

such that $V^*_{|_{C_i}}(x) = V_i^*(x)$ defined in (28) and $h^*_{|_{C_i}}(x) = h_i^*(x)$ defined in (29), and $v^*_{|_{C_i}}(x) = v_i$.

With this choice, the reconstruction of the conserved variables are defined by

$$P_i^h(x) = h_i^*(x),$$
$$P_i^{hu}(x) = (hu)_i,$$
$$P_i^{hv}(x) = h_i^*(x)v_i^*(x).$$

The second-order reconstruction is defined similarly. First, a standard second-order reconstruction for v_i is considered, that is

$$P_i^v(x) = v_i + \sigma_{vi}(x - x_i), \tag{30}$$

where

$$\sigma_{v i} = \text{minmod}\left(\frac{v_i - v_{i-1}}{\Delta x}, \frac{v_{i+1} - v_i}{\Delta x}\right).$$

Next, we define the local steady-state $v_i^*(x)$ as the previous reconstruction. That is $v_i^*(x)$ is defined on the stencil S_i as $(v_i^*)_{|C_l}(x) = P_l^v(x)$, $l \in \{i-1, i, i+1\}$. Note that, in general, $v_i^*(x)$ is not a continuous function on the stencil S_i.

We compute $V^*(x)$, a continuous primitive of $v^*(x)$, where $v^*(x)_{|C_i} = v_i^*(x)$. As in the previous case, we define $V^*(x)$ at each cell C_i as follows:

$$V_i^*(x) = v_i(x - x_i) + \sigma_{v i}\frac{(x - x_i)^2}{2} + K_i, \tag{31}$$

where K_i is a constant that it is defined such that $V_{i-1}^*(x_{i-1/2}) = V_i^*(x_{i-1/2})$. As previously, setting $K_0 = 0$, we define

$$K_i = \frac{v_i + v_{i-1}}{2}\Delta x - (\sigma_{v i} - \sigma_{v i-1})\frac{\Delta x^2}{8} + K_{i-1}, \quad i = 1, \dots \tag{32}$$

Again, once $V_i^*(x)$ is computed, then $h_i^*(x)$ is defined by (29). Again $(hu)_i^*(x) = 0$. As in the first-order case, the approximate steady states are defined by:

$$h^*(x) = \frac{E}{g} - z(x) + \frac{f}{g}V^*(x),$$
$$u^* = 0,$$

such that $V_{|C_i}^*(x) = V_i^*(x)$ defined in (31) and $h_{|C_i}^*(x) = h_i^*(x)$ defined in (29), and $v_{|C_i}^*(x) = P_i^v(x)$.

In this case, the reconstruction operators of the conserved variables read as follows:

$$P_i^h(x) = h_i^*(x) + Q_i^h(x),$$
$$P_i^{hv}(x) = h_i^*(x)v_i^*(x) + Q_i^{hv}(x),$$
$$P_i^{hu}(x) = Q_i^{hu}(x),$$

where $Q_i^h(x)$ and $Q_i^{hv}(x)$ are standard 2nd order reconstructions applied to the fluctuations of h and hv with respect to the local steady states h_i^* and $h_i^*v_i^*$, respectively, and $Q_i^{hu}(x)$ is a standard reconstruction operator applied to the cell averages hu_i on the stencil S_i, as $hu^* = 0$.

Remark 3.1. Note that in this case, v^* is a non-smooth approximation of v, although h^* is continuous. Therefore we cannot say that the numerical scheme based on this reconstruction procedure is *exactly well-balanced* for the steady state for $u = 0$ and v, an arbitrary function, but, one could expect that the numerical method exactly preserves the approximate steady states, previously characterised. Moreover, as pointed out in Remark 2.2, we cannot expect that the numerical scheme (12) with an arbitrary numerical flux can preserve such approximate non-smooth steady states. It can be easily checked that if the HLL (see [32]) Riemann solver is used, those are not preserved. Instead, any numerical solver that can preserve contact discontinuities associated with the linear field associated with the eigenvalue $\lambda = u$, then Theorem 2.1 remains true. In particular, we can consider HLLC Riemann solver (see for example [35,36,27,1]).

Another possibility that allows the use of any consistent numerical flux is to consider a smooth approximation of the velocity field v^*. Thus, for first and second-order numerical methods, we could assume a continuous piece-linear approximation of v^* at every interval $[x_i, x_{i+1}]$, that is $v^*(x_i) = v_i$. Note that it is necessary to extend v^* at the first and last cells to define v^* in the complete domain. Now, it is possible to compute a primitive of v^* denoted by V^*. Once $V^*(x)$ is obtained, $h^*(x)$ is given by

$$h^*(x) = \frac{E}{g} - z(x) + \frac{f}{g}V^*(x).$$

Finally, the reconstruction operators of the conserved variables are again defined as

$$P_i^h(x) = h_i^*(x) + Q_i^h(x),$$
$$P_i^{hv}(x) = h_i^*(x)v_i^*(x) + Q_i^{hv}(x),$$
$$P_i^{hu}(x) = Q_i^{hu}(x),$$

where $Q_i^h(x)$ and $Q_i^{hv}(x)$ are standard second-order reconstruction operators applied to the fluctuations of h and hv with respect to the local steady states h^* and h^*v^* at each cell respectively, and $Q_i^{hu}(x)$ is a standard reconstruction operator applied to the cell averages hu_i on the stencil S_i, as $hu^* = 0$. Note that Q reduces to a constant in the case of a first-order scheme.

Remark 3.2. Note that the main difference between the case $u \neq 0$ and $u = 0$ is the definition of $V^*(x)$. Once $V^*(x)$ is defined, the computation of h^* and the reconstruction procedure remains equal. Therefore, from the practical point of view, according to u, we consider the corresponding definition of V^* and the rest remains the same.

The choice of the functional form of v^* and h^* will also affect the boundary treatment and how the values in the grid might be extended to boundaries.

3.2. High-order CWENO reconstruction

In this section, we are going to give a brief description of the general well-balanced reconstruction. For a detailed derivation, we refer the reader to Appendix A where an elaborated example for the third-order CWENO is also provided.

The main difficulty in this case is that we cannot obtain a direct value of point values from the cell averages. Therefore E_i cannot be set directly from the cell averages and a non-linear problem that involves equations (19)-(21) and the one corresponding the cell average of h^* at cell C_i must be solved at each quadrature point.

Let us consider a quadrature formula with n points $\{x_i^p\}_{p=1,\cdots n}$, and their corresponding weights $\{\alpha_i^p\}_{i=1,\cdots p}$. Taken into account that v_0 in (20) is related with the cell average of $(hv)_i$ by

$$v_0 = \frac{(hv)_i + f\sum_{p=1}^{n} f\,\alpha_i^p x_i^p h^*(x_i^p)}{h_i}. \tag{33}$$

Now, replacing $V^*(x)$ defined in (21) into (19), the non-linear problems to solve are the following:

$$g_0(h_i^{*,1},\dots,h_i^{*,n},E_i) = \sum_{p=1}^{n} \alpha_p h_i^{*,p} - h_i,$$

$$g_p(h_i^{*,1},\dots,h_i^{*,n},E_i) = \left(gz(x_i^p) - f\left(-\frac{f}{2}\left(x_i^p\right)^2 + \left(\frac{(hv)_i + f\sum_{l=1}^{n}\alpha_p h_i^{*,l} x_i^p}{h_i} \right) x_i^p \right) - E_i \right) (h_i^{*,p})^2$$
$$+ g(h_i^{*,p})^3 + \frac{(hu)_i}{2}, \quad p = 1,\dots,n,$$

where $h_i^{*,p} = h_i^*(x_i^p)$, $p = 1,\cdots,n$. Once the non-linear system is solved, then h_i^* at the quadrature points are computed as well as the level of energy E_i. Now the values of the steady states at the intercells and all the other points of interest in the stencil could be computed as in the first and second-order scheme.

For the case $u = 0$ we could extend both approaches previously defined, one where $v^*(x)$ is discontinuous based on the use of standard reconstructions of hv and h to compute the point values approximations of v at the cell C_i and a continuous approximation based on a smooth reconstruction of v in the complete domain based on the definition of a spline computed on a given set of points, as in the first approximation.

Nevertheless in this work, we have considered that v^* is given by a piecewise linear approximation of v^*, such that it is constant in all quadrature points that are in the same cell, that is v^* is constant in $[x_i^0, x_i^p]$ and linear in $[x_i^p, x_{i+1}^0]$. With this choice, v^* is only second-order accurate for those steady states ($u = 0$). In any case, for non-zero steady states, the scheme is exactly well-balanced and the scheme is high-order, with the accuracy of the CWENO scheme for arbitrary smooth non-steady states.

Regarding the water height positivity preservation, we can follow [23] to prove this property for the first-order scheme. In the case of the high-order scheme, it is much more difficult to prove this property. However, in [42] they propose a procedure that might be successful in verifying the water height positivity preservation for a higher-order scheme. This will be used in future work.

4. Numerical experiments

In this section, some numerical experiments to assess the good properties of the developed numerical schemes, are presented. We consider 1st, 2nd and 3rd-order WB and non-WB methods. 1st, 2nd and 3rd-order methods are denoted by $\mathcal{O}(1)$, $\mathcal{O}(2)$ and $\mathcal{O}(3)$, respectively. MUSCL ([40]) reconstruction is used for the second-order methods, while CWENO ([25]) reconstruction is employed for the third-order methods.

As pointed out before, the main difference between the case $u \neq 0$ and $u = 0$ is the definition of V^*. Once this is determined, the same procedure is applied in all cases. To avoid the use of conditionals in the definition of the well-balanced reconstruction, we consider a convex combination of V_0^* and V^*, the first one corresponding to $u = 0$ and the second one for $u \neq 0$. In particular, we define

$$V^* = (1 - \beta(u))V_0^* + \beta(u)V^*,$$

where $\beta(u)$ is the sigmoid function:

$$\beta(u) = \frac{1}{1 + exp\left[-C_2\left(|u| - C_1\right)\right]}, \tag{34}$$

with $C_1 = 5 \cdot 10^{-14}$ and $C_2 = 1 \cdot 10^{15}$. With this choice, determined experimentally, $\beta = 0$ when u is close to zero and $\beta = 1$ in any other case. This convex combination is applied in every numerical experiment. In numerical experiments 4 and 5 the value of β switches from 0 to 1 as explained in the latter.

For the numerical flux, we consider the HLL (see [32]) and HLLC (see [37,27,1]) Riemann solvers. The stability condition for the scheme reads:

$$\Delta t \leq CFL \min_i \left(\frac{\Delta x}{\max\{|\lambda_{i,L}|, |\lambda_{i,R}|\}} \right),$$

where $CFL < 1$ and

$$\lambda_{i,L} = \min_{q=hu} \left(\frac{q^-_{i+1/2}}{h^-_{i+1/2}} - \sqrt{g h^-_{i+1/2}}, \frac{\frac{q^-_{i+1/2}}{h^-_{i+1/2}} \sqrt{h^-_{i+1/2}} + \frac{q^+_{i+1/2}}{h^+_{i+1/2}} \sqrt{h^+_{i+1/2}}}{\sqrt{h^-_{i+1/2}} + \sqrt{h^+_{i+1/2}}} - \sqrt{0.5 g (h^+_{i+1/2} + h^-_{i+1/2})} \right),$$

$$\lambda_{i,R} = \max_{q=hu} \left(\frac{q^+_{i+1/2}}{h^+_{i+1/2}} + \sqrt{g h^+_{i+1/2}}, \frac{\frac{q^-_{i+1/2}}{h^-_{i+1/2}} \sqrt{h^-_{i+1/2}} + \frac{q^+_{i+1/2}}{h^+_{i+1/2}} \sqrt{h^+_{i+1/2}}}{\sqrt{h^-_{i+1/2}} + \sqrt{h^+_{i+1/2}}} + \sqrt{0.5 g (h^+_{i+1/2} + h^-_{i+1/2})} \right),$$

are the wave speed estimates at the intercell $i + 1/2$.

The water regime for the numerical experiments is determined by

$$R_o = \frac{V}{fL}, \; B_u = \frac{R_d^2}{L^2}, \; R_d = \frac{\sqrt{gH}}{f},$$

which are the Rossby number, Burgers number and Rossby formation radius respectively. Also, the time scale is defined by characteristic time which is

$$T_C = \begin{cases} \frac{L}{\sqrt{gH}} & u = 0, \\ \frac{L}{V + \sqrt{gH}} & u \neq 0. \end{cases}$$

Where V is the mean of the horizontal velocity, L is the length of the domain and H is the mean of water height. This characteristic time gives an idea of how long it takes for a perturbation to leave the spatial domain.

4.1. Numerical experiment 1

For this numerical experiment, we consider the moving steady-state proposed in [26]. This is

$$h^*(x) = e^{2x},$$
$$u^*(x) = \frac{e^{-2x}}{2},$$
$$v^*(x) = -fx.$$
$$z(x) = -\frac{f^2}{2} x^2 - e^{2x} - \frac{e^{-4x}}{8}.$$

The numerical experiment will be initialised under this stationary state. While we consider $f = g = 1$, a number $CFL = 0.8$, final time $T = 5$ and domain $x \in [0, 1]$. We consider Neumann boundary conditions, for all $t > 0$:

- On the left boundary $h'(0,t) = 2$, $hu'(0,t) = 0$, $hv'(0,t) = -f$.
- On the right boundary $h'(1,t) = 2e^2$, $(hu)'(1,t) = 0$, $(hv)'(1,t) = -3fe^2$.

For this case we compute $R_d = 1.7873$, $B_u = 3.1945$ and $R_o = 0.2162$. Finally, the characteristic time is $T_C = 0.4991$ which means that the simulation is carried out for more than a ten times larger time.

Simulating for $N = 25, 50, 100, 200, 400$ and the well-balanced schemes, we show the results of the error for each component in the Table 1. The expected behaviour of the results is observed: the errors are of the order of the machine error. For the third-order scheme, it is important to notice that the errors are affected by the Newton solver of the non-linear system. It is used to determine the stationary solutions every timestep and at every stencil with errors of the order of 10^{-15}. This results in an accumulation of small errors that will affect the final error. When using a non well-balanced scheme the order of the scheme is recovered.

Table 1
Errors for the first numerical experiment under the L_1-norm. We show the results for different numbers of cells at time $T = 5$ for the first, second and third-order schemes and every conserved variable.

Variable Reconstruction	h			hu			hv		
N	$\mathcal{O}(1)$	$\mathcal{O}(2)$	$\mathcal{O}(3)$	$\mathcal{O}(1)$	$\mathcal{O}(2)$	$\mathcal{O}(3)$	$\mathcal{O}(1)$	$\mathcal{O}(2)$	$\mathcal{O}(3)$
25	0e+00	0e+00	5e-14	2e-16	6e-16	1e-14	1e-15	7e-16	5e-14
50	4e-16	0e+00	9e-14	3e-15	3e-16	7e-15	4e-14	6e-16	1e-13
100	1e-15	0e+00	3e-13	6e-15	2e-16	7e-14	9e-14	4e-16	2e-13
200	1e-14	0e+00	8e-13	4e-14	5e-16	2e-13	4e-13	4e-16	5e-13
400	1e-17	1e-17	2e-12	3e-16	3e-16	6e-13	2e-15	4e-16	9e-13

Table 2
Errors under the L_1 norm for each conserved variable at time $T = 5$ for the well-balanced (WB) and non-well-balanced (NWB) for $\mathcal{O}(3)$ schemes.

N	h component			hu component			hv component		
	WB	NWB	$\mathcal{O}$(NWB)	WB	NWB	$\mathcal{O}$(NWB)	WB	NWB	$\mathcal{O}$(NWB)
25	1e-15	3e-07	-	2e-16	1e-07	-	2e-16	4e-07	-
50	2e-15	3e-08	3.12	4e-16	1e-08	3.12	4e-16	5e-08	3.07
100	5e-15	4e-09	3.06	8e-16	1e-09	3.06	9e-16	6e-09	3.04
200	8e-15	4e-10	3.03	1e-15	2e-10	3.03	2e-15	7e-10	3.02
400	2e-14	5e-11	3.02	3e-15	2e-11	3.02	3e-15	9e-11	3.01

4.2. Numerical experiment 2

For this numerical experiment, we initialize the problem with a stationary solution of the shallow-water system with Coriolis source terms described by:

$$h^*(x) = \frac{2+\sin x}{2+\cos x},$$
$$u^*(x) = \sqrt{g}\frac{2+\cos x}{2+\sin x},$$
$$v^*(x) = -fx,$$
$$z(x) = \frac{1}{2g} - \frac{f^2}{2g}x^2 - \frac{2+\sin x}{2+\cos x} - \frac{1}{2}\left(\frac{2+\cos x}{2+\sin x}\right)^2.$$

Where $g = 1$ and $f = 1$ are the gravity and Coriolis constants, respectively. We choose the domain of the problem $x \in [0, 0.5]$, a final time $T = 5$ and the CFL is fixed to 0.7. For the boundary conditions, we have considered Neumann boundary conditions based on the derivatives of the stationary solution on the boundaries. For this case $R_d = 0.8714$, $Bu = 3.0375$ and $R_0 = 2.6483$. The characteristic time is $T_C = 0.2277$ which means that $T >> T_C$.

In Table 2 we show the comparison between the solutions, calculated with the third-order scheme, for this numerical experiment and the stationary solutions. In this table, it is shown that the scheme is exactly WB for the chosen stationary solution looking at the order of the errors. The accuracy remains the same for the rest of the schemes.

4.3. Numerical experiment 3

For the third numerical experiment, we consider a non-linear combination of two stationary solutions similar to the ones described in the first numerical experiment. For the non-linear combination, we consider the sigmoid function:

$$\sigma(x) = \frac{1}{e^{20(1-x)}+1}$$

Then, we consider the following water depth and horizontal velocity

$$h_1(x) = e^{2x}, \qquad h_2(x) = e^{1x},$$
$$u_1(x) = 0.5e^{-2x}, \qquad u_2(x) = 0.2e^{-x}.$$

Then, we build the functions

$$h_0(x) = (1-\sigma(x))h_1(x) + \sigma(x)h_2(x),$$
$$u_0(x) = (1-\sigma(x))u_1(x) + \sigma(x)u_2(x),$$
$$(hu)_0(x) = h_0(x)u_0(x),$$

Table 3
First-order reconstruction errors and convergence rate concerning a reference solution. The results are shown for the conserved variables and the well-balanced (WB) and non-well-balanced (NWB) schemes.

Var	h				hu				hv			
Rec	WB		NWB		WB		NWB		WB		NWB	
N	E(N)	$\mathcal{O}$	E(N)	$\mathcal{O}$	E(N)	$\mathcal{O}$	E(N)	$\mathcal{O}$	E(N)	$\mathcal{O}$	E(N)	$\mathcal{O}$
16	8e-02	0.00	2e+02	0.00	7e-02	0.00	3e+00	0.00	1e-01	0.00	5e+02	0.00
32	4e-02	0.82	4e-01	8.99	5e-02	0.82	3e-01	8.99	5e-02	0.82	9e-01	8.99
64	2e-02	1.03	2e-01	1.06	3e-02	1.03	2e-01	1.06	2e-02	1.03	4e-01	1.06
128	1e-02	0.80	8e-02	1.01	2e-02	0.80	8e-02	1.01	1e-02	0.80	2e-01	1.01
256	7e-03	0.81	4e-02	0.98	1e-02	0.81	4e-02	0.98	7e-03	0.81	1e-01	0.98
512	4e-03	0.82	2e-02	0.98	7e-03	0.82	2e-02	0.98	4e-03	0.82	6e-02	0.98
1024	2e-03	0.85	1e-02	0.98	4e-03	0.85	1e-02	0.98	2e-03	0.85	3e-02	0.98

Table 4
Second-order reconstruction errors and convergence rate concerning a reference solution. The results are shown for the conserved variables and the well-balanced (WB) and non-well-balanced (NWB) schemes.

Var	h				hu				hv			
Rec	WB		NWB		WB		NWB		WB		NWB	
N	E(N)	$\mathcal{O}$	E(N)	$\mathcal{O}$	E(N)	$\mathcal{O}$	E(N)	$\mathcal{O}$	E(N)	$\mathcal{O}$	E(N)	$\mathcal{O}$
16	7e-02	0.00	1e-01	0.00	4e-02	0.00	1e-01	0.00	1e-01	0.00	3e-01	0.00
32	3e-02	1.11	4e-02	1.28	2e-02	1.11	4e-02	1.28	5e-02	1.11	9e-02	1.28
64	1e-02	1.63	1e-02	1.67	1e-02	1.63	1e-02	1.67	1e-02	1.63	3e-02	1.67
128	4e-03	1.51	4e-03	1.60	4e-03	1.51	5e-03	1.60	4e-03	1.51	9e-03	1.60
256	1e-03	1.70	1e-03	1.73	1e-03	1.70	2e-03	1.73	1e-03	1.70	3e-03	1.73
512	3e-04	1.86	3e-04	1.87	4e-04	1.86	4e-04	1.87	3e-04	1.86	7e-04	1.87
1024	9e-05	1.84	9e-05	1.88	1e-04	1.84	1e-04	1.88	9e-05	1.84	2e-04	1.88

Table 5
Third-order reconstruction errors and convergence rate concerning a reference solution. The results are shown for the conserved variables and the well-balanced (WB) and non-well-balanced (NWB) schemes.

Var	h				hu				hv			
Rec	WB		NWB		WB		NWB		WB		NWB	
N	E(N)	$\mathcal{O}$	E(N)	$\mathcal{O}$	E(N)	$\mathcal{O}$	E(N)	$\mathcal{O}$	E(N)	$\mathcal{O}$	E(N)	$\mathcal{O}$
16	3e-02	0.00	5e-02	0.00	6e-02	0.00	2e-01	0.00	3e-02	0.00	2e-01	0.00
32	8e-03	1.87	1e-02	1.80	2e-02	1.87	4e-02	1.80	9e-03	1.87	6e-02	1.80
64	3e-03	1.42	5e-03	1.59	5e-03	1.42	1e-02	1.59	3e-03	1.42	2e-02	1.59
128	9e-04	1.72	1e-03	1.78	1e-03	1.72	3e-03	1.78	7e-04	1.72	4e-03	1.78
256	2e-04	2.19	3e-04	2.09	3e-04	2.19	7e-04	2.09	1e-04	2.19	1e-03	2.09
512	3e-05	2.65	6e-05	2.35	4e-05	2.65	2e-04	2.35	2e-05	2.65	2e-04	2.35
1024	4e-06	2.88	1e-05	2.35	6e-06	2.88	4e-05	2.35	2e-06	2.88	3e-05	2.35

$$(hv)_0(x) = -fxh_0(x),$$
$$z(x) = -0.5f^2x^2 - h_0(x) - \frac{1}{2g}u_0^2(x).$$

We initialise the scheme with (h_0, hu_0, hv_0) with z as the bottom topography. In this case, we expect the exactly well-balanced scheme to be well-balanced in the domain $\mathbb{R} - \{x : |\, x-1 \,| > \delta\}$ for a big enough δ at $t = 0$.

For the experiment setup, we consider $f = g = 1$, a domain $x \in [0, 3]$, a CFL number of 0.8, $T = 0.5$ and non-reflective boundary conditions. The reference solution is calculated using a very fine mesh consisting of 2^{13} finite volumes, and the third-order non well-balanced scheme. The numerical solutions for the 1st, 2nd and 3rd order, WB and non-WB schemes, computed using $N = 2^i$ for $i = 4, 5, 6, 7, 8, 9, 10$ cells, are compared against the aforementioned reference solution. For this case $R_d = 2.6212$, $Bu = 0.7634$, $R_0 = 0.0311$ and $T_C = 1.1052$. Here it is not relevant that $T < T_C$ because we are testing the convergence rate and not the well-balanced property.

Tables 3, 4 and 5 show the errors and convergence rate for the first, second and third-order schemes respectively under the L_1 norm. The results show that the rate of convergence is recovered in the well-balanced schemes when the solution is not globally stationary. What is more, we observe that the error committed by the well-balanced scheme is, in general, lower than the one committed by the non-well-balanced scheme. This behaviour is especially manifested in the hv variable where the error of the well-balanced scheme is one order of magnitude more precise than the error for the non-well-balanced scheme.

Table 6
Errors committed for the $\mathcal{O}(3)$ scheme under L_1 norm for the fourth numerical experiment. Initial data given by the continuous stationary solution (35)-(37).

N	h component		hu component		hv component	
	WB		WB		WB	
	E_N	O_N	E_N	O_N	E_N	O_N
25	2e-01	-	4e-02	-	4e-01	-
50	3e-02	2.43	8e-03	2.35	6e-02	2.66
100	3e-03	3.08	1e-03	3.03	8e-03	3.02
200	4e-04	3.18	1e-04	3.14	9e-04	3.06
400	4e-05	3.10	1e-05	3.10	1e-04	3.01

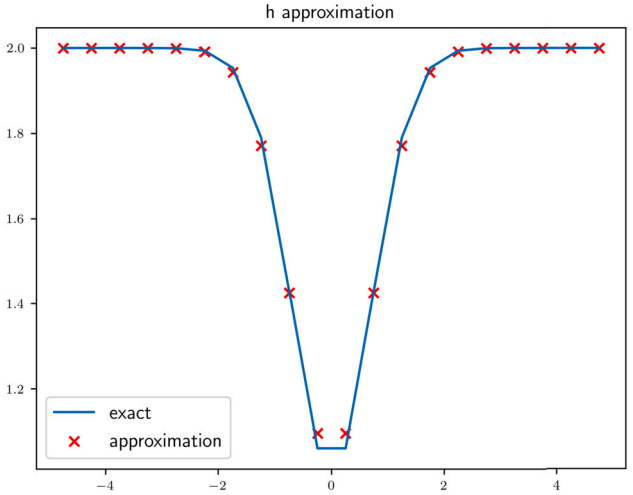

Fig. 1. Water depth of the discrete stationary solution approximating the continuous stationary solution (35)-(37) with $N = 20$.

4.4. Numerical experiment 4

In this case, we consider the steady-state proposed in [16] with $u = 0$ given by:

$$h^*(x) = \frac{2}{g} - e^{-x^2}, \tag{35}$$

$$u^*(x) = 0, \tag{36}$$

$$v^*(x) = \frac{2g}{f} x e^{-x^2}. \tag{37}$$

We choose $f = g = 1$, $\Omega = [-5, 5]$, $CFL = 0.8$, null flux across the boundaries and a final time $T = 10$ and it is simulated with the $\mathcal{O}(2)$ and $\mathcal{O}(3)$ schemes. For this case, we have $R_d = 1.3501$, $Bu = 0.0182$ and $R_0 = 0$. The reference time is $T_C = 7.4069$.

We first consider as initial conditions, those corresponding to the use of the exact expression of the steady state integrated at each cell. In this case, we cannot expect that our numerical scheme exactly preserves this initial steady state and it is what we observe in Table 6, but we recover the third-order accuracy. Here the switch (34) starts with a value of 0, which means that $u^*(x) = 0$. After the first computation, as $v^*(x)$ is not a well-prepared steady solution, the value of β switches to 1 which means that $u^*(x) \neq 0$.

Now, we can consider a discrete steady state that is an approximation of the previous steady state and that is preserved for the numerical scheme. Thus, we follow the procedure described previously to compute a well-prepared initial condition whose velocity v is a piece-wise linear approximation of this initial steady state. In Fig. 1 we show the approximation of h^* for $N = 20$. As expected the scheme can exactly preserve this discrete steady state (see Table 7) and errors are of the order of the machine accuracy. Finally, we compute the errors of the discrete steady states that are preserved by the second and third-order numerical scheme and as expected both are second-order (see Table 8). Note that those results could be improved easily by considering either non-smooth reconstructions of v^* in combination with the HLLC Riemann solver or a continuous approximation of v^* using third-order spline approximations for v^*.

Finally, we could adapt the previous numerical scheme to preserve exactly those steady states by considering a general family of steady states with the following functional form:

$$h(x) = C - \frac{f}{2g} K e^{-x^2},\ u(x) = 0,\ v(x) = K x e^{-x^2},$$

Table 7
Errors for the well-balanced $\mathcal{O}(2)$ and $\mathcal{O}(3)$ schemes under the L_1 norm. The scheme is initialized with the well-prepared discrete stationary solution approximating (35)-(37).

	h		hu		hv	
N	$\mathcal{O}(2)$	$\mathcal{O}(3)$	$\mathcal{O}(2)$	$\mathcal{O}(3)$	$\mathcal{O}(2)$	$\mathcal{O}(3)$
20	9e-15	2e-14	1e-14	2e-14	1e-15	3e-15
40	2e-14	1e-13	5e-14	2e-14	8e-15	2e-14
80	5e-14	8e-14	1e-14	2e-14	1e-14	2e-14
160	3e-14	9e-14	1e-14	3e-14	2e-14	4e-14
320	6e-14	4e-13	2e-13	7e-14	5e-14	8e-14

Table 8
Errors and order of convergence for the well-prepared continuous initial condition concerning the exact stationary initial condition.

	N	20	40	80	160	320
Second-order scheme	E	7e-2	2e-2	4e-3	1e-3	3e-4
	O	-	1.89	2	2	2
Third-order scheme	E	7e-2	2e-2	4e-3	1e-3	3e-4
	O	-	1.95	2.01	2	2

Table 9
Errors committed under the L_1 norm for the exactly well-balanced schemes for a family of exponential functions. The errors are shown for the $\mathcal{O}(3)$ scheme.

N	h	hu	hv
20	3e-14	1e-14	1e-14
40	8e-14	1e-14	5e-14
80	2e-13	2e-14	1e-13
160	4e-13	3e-14	2e-13
320	7e-13	5e-14	5e-13

where C and K are two constants to be determined. Locally, in the i-th cell, those values are determined by solving the non-linear system of equations:

$$h_i = C - \frac{f}{2g}K \int_{x_{i-1/2}}^{x_{i+1/2}} e^{-x^2} dx,$$

$$hv_i = CK \int_{x_{i-1/2}}^{x_{i+1/2}} xe^{-x^2} dx - \frac{f}{2g}K^2 \int_{x_{i-1/2}}^{x_{i+1/2}} xe^{-2x^2} dx.$$

In Table 9 we show the errors for this exactly well-balanced $\mathcal{O}(3)$ scheme, where all the errors are a result of solving the previous non-linear system of equations in every cell and every time step.

Thus, in this case, it is possible to combine the general procedure defined for non-zero steady states with the particular choice of this family of steady states for $u = 0$.

4.5. Numerical experiment 5: jet

In this numerical test, we check the ability of the numerical scheme to approximate non-steady states. In particular, we consider a jet initial condition (see [9,16]). The initial condition is written as follows:

$$h(x) = H,$$

$$u(x) = 0,$$

$$v(x) = HV \frac{(1 + \tanh(4x/L + 2))(1 - \tanh(4x/L + 2))}{(1 + \tanh 2)^2}.$$

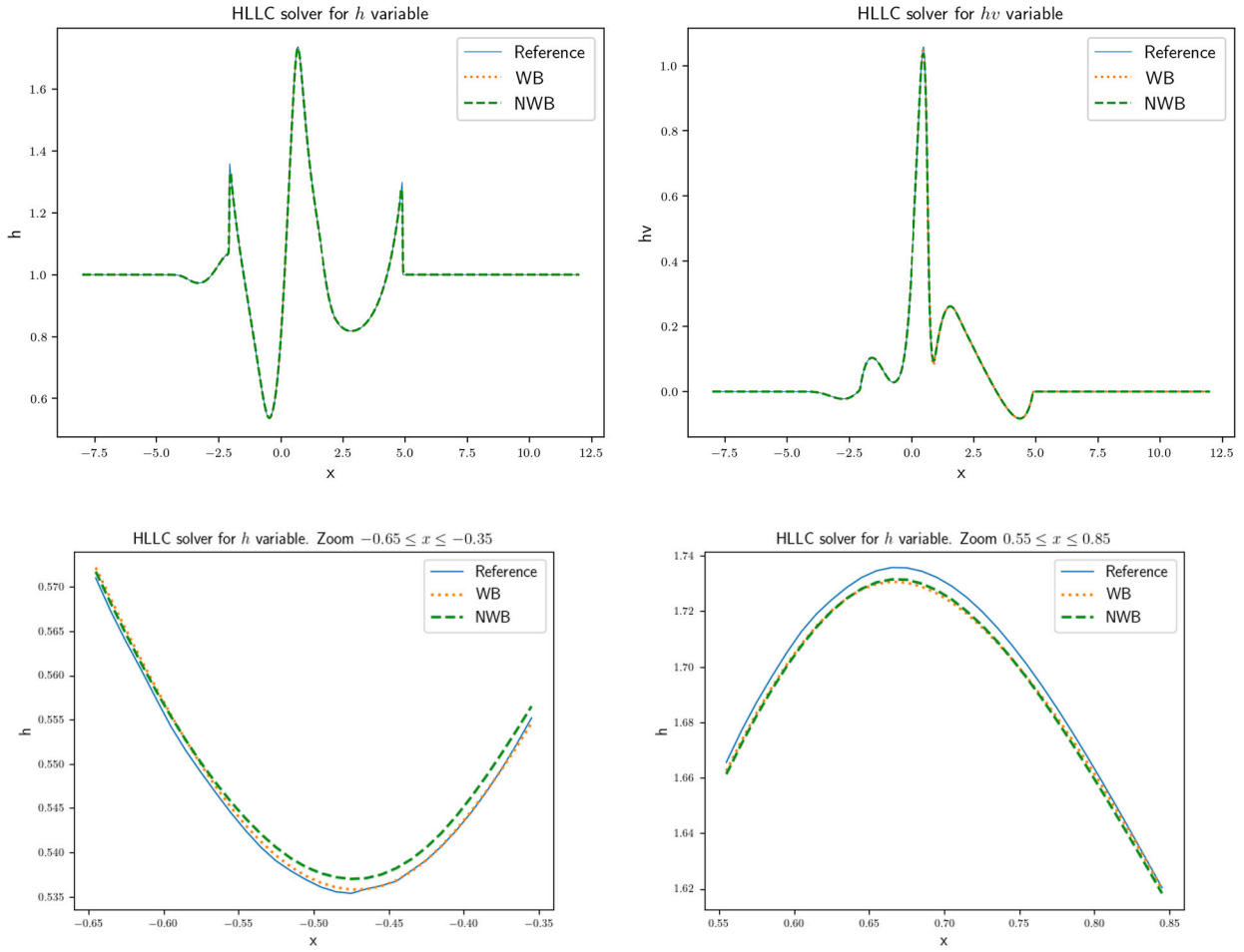

Fig. 2. Water depth (top left), tangential momentum (top right) for the jet formation at time $T = 2\pi$, zoom for the water depth for $x \in [-0.65, -0.35]$ and $x \in [0.55, 0.85]$ (bottom left and right respectively). Comparison between a reference solution computed with $N = 20000$ and the well-balanced and not well-balanced second-order schemes.

We consider $B_u = 0.25$, $R_o = 1$, $CFL = 0.9$ as it was set in [16]. With these values, we fix $H = L = V = 1$, then $g = 0.25$ and $f = 1$. We consider a domain $x \in [-8, 12]$ and a final time $T = 2\pi/f$. We also consider $N = 2000$ to satisfy $R_d/\Delta x = 50$ as it is studied in the literature. In this case, the definition of V is set by the problem and not by the mean of the horizontal velocity.

In Fig. 2 we compare a reference solution computed with $N = 20000$ points and the WB and non-WB second-order schemes for the h and hv variables with an HLLC solver. In this figure, we also represent two zooms in regular regions of the jet. Both figures show how the well-balanced scheme performs slightly better than the non-well-balanced scheme. In Fig. 3 we plot the time evolution of the jet for different times under the same numerical experiment for the well-balanced scheme. We observe how the behaviour of our scheme is similar to the one presented in the literature [16]. Finally, in Fig. 4 we plot the balance between the Coriolis and Gravity source terms. As we can see, the balance is not reached due to the numerical error committed. In this numerical example, our scheme performs equally to the schemes found in the literature. This is because the jet is an extreme case (with shock production) far away from the stationary solutions we study in this work.

Data availability

No data was used in this research. Code can be shared within request.

Acknowledgements

Manuel J. Castro has been funded by FEDER and the Spanish Government through the coordinated Research project RTI2018-096064-B-C1. Also, this research has been partially funded by MCIN/AEI/10.13039/501100011033 and by the "European Union NextGenerationEU/PRTR" through the grant PDC2022-133663-C21 and by MCIN/AEI/10.13039/50110001103 and by "ERDF A way of making Europe", by the "European Union" through the grant PID2022-137637NB-C21. The other authors' research has been

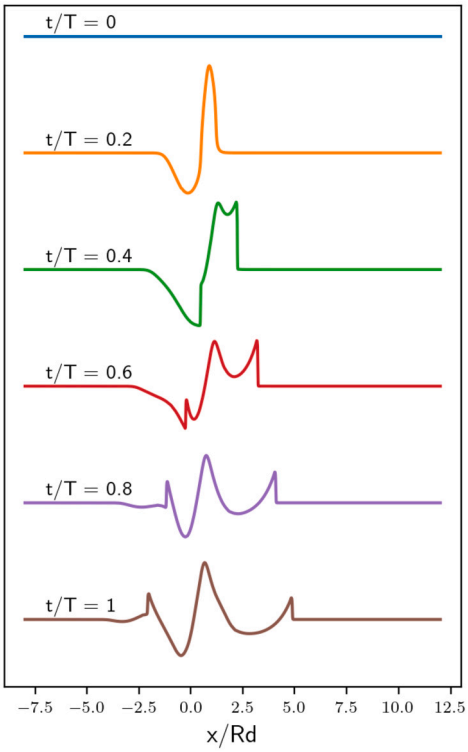

Fig. 3. Water depth evolution of the jet computed with a final time of $T = 2\pi$.

funded by the Spanish MINECO under research project number PID2022-141058OB-I00 and by the grant ED431G 2019/01 of CITIC, funded by Consellería de Educación, Universidade e Formación Profesional of Xunta de Galicia and FEDER.

Appendix A. Determining the local stationary solutions for a 2n-1 CWENO reconstruction

In section 3 we described how to design an exactly well-balanced reconstruction that preserves the solutions of system (15)-(17) for $hu \neq 0$ the stationary solutions read as:

$$(hu)^*(x) = C, \tag{38}$$

$$\frac{(u^*(x))^2}{2} + g\left(h^*(x) + z(x) - fV(x)\right) = E \tag{39}$$

$$v^* = -fx + v_0, \tag{40}$$

$$V(x) = -\frac{f}{2}x^2 + v_0 x, \tag{41}$$

where C, E and v_0 are constants.

In this section, we are providing a general technique to obtain an exactly well-balanced scheme for this stationary well-balanced solution using a $2n-1$ order CWENO reconstruction procedure. In this kind of reconstruction, we have the following ingredients:

1. The highest polynomial degree is $2n-2$.
2. The stencil must have $2n-1$ cells.
3. To preserve the order, we need a quadrature formula with $2n-1$ accuracy. The optimal formula can be chosen with the Legendre polynomials leading to an exact $2n-2$ polynomial precision. If the CWENO reconstruction procedure has an error of Δx^{2n-1}, the quadrature formula must be, at least, precise for polynomials of degree $2n-1$, which means that it has n or more quadrature points. We write this formula as follows:

$$\int_{x_{i-1/2}}^{x_{i+1/2}} f(x)dx \approx \sum_{p=1}^{n} \alpha_i^p f(x_i^p),$$

where α_i^p are the linear weights and x_i^p are the quadrature points.

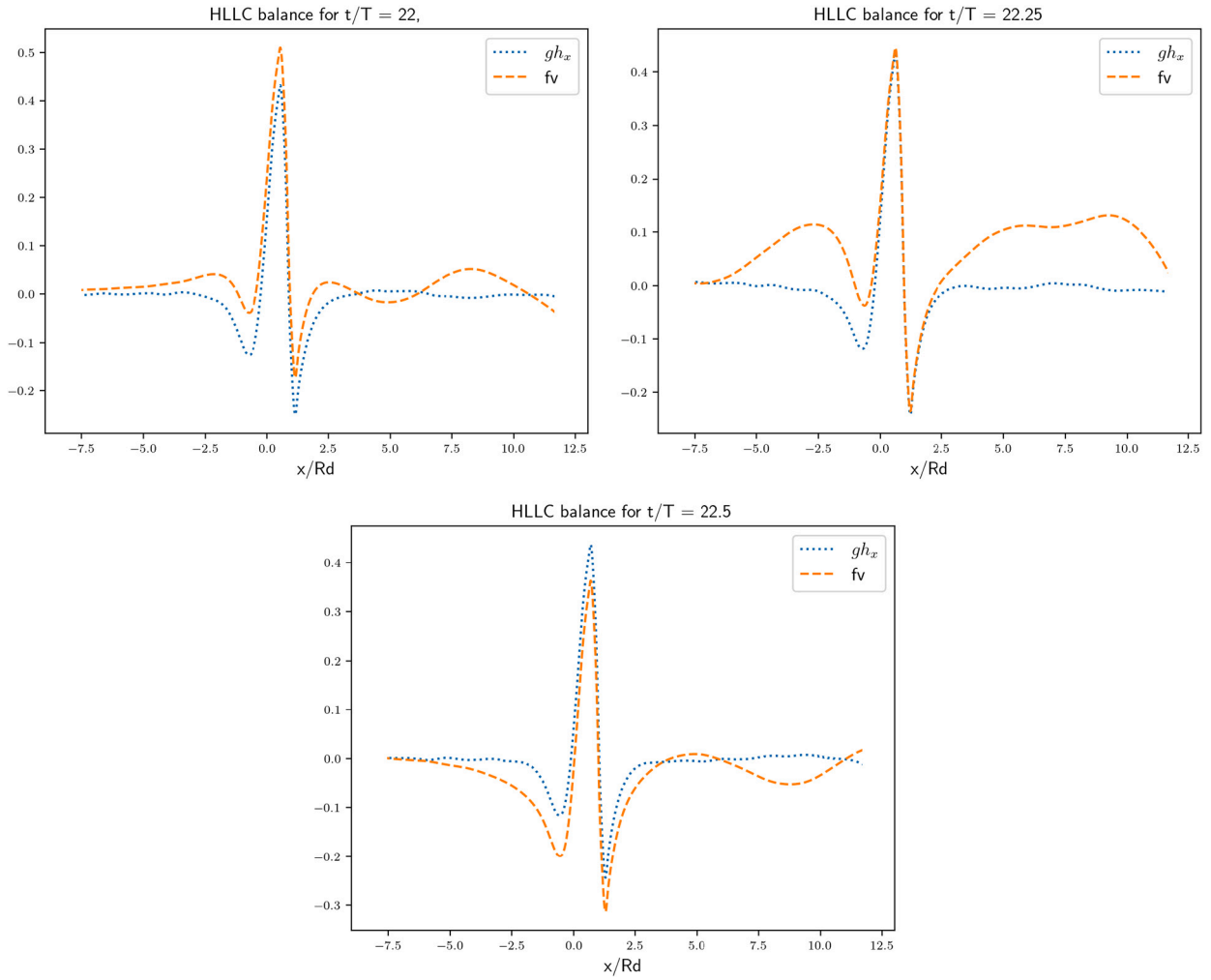

Fig. 4. Balance between Coriolis and Gravity source terms for long times under the well-balanced scheme.

To obtain an exactly well-balanced reconstruction, we need to be able to obtain point-wise values of the local stationary solution in each stencil $\mathcal{S}_i$. In this case, the points of interest can be classified into two families:

1. Point values at the quadrature points $\{x_i^p\}_{p=1}^n$ for each cell in the stencil $\mathcal{S}_i = \{C_{i-(n-1)}, \dots, C_{i+(n-1)}\}$. These values allow us to calculate the averages of the stationary solutions for every cell in the stencil, and the integral of the source term for the centre cell C_i.
2. Two point values in the intercells $x_{i\pm 1/2}$ in order to evaluate the fluxes.

This yields a total of $(2n-1)n+2$ points of interest in each stencil.

From (38)-(41) we can derive the following system of equations that must be satisfied by the stationary solution in each stencil $\mathcal{S}_i$

$$hu^*(x_k) = (hu)_i, \tag{42}$$

$$v^*(x_k) = -f x_k + v_i, \tag{43}$$

$h^*(x_k)$ is root of

$$g(h^*)^3(x_k) + \left(g z(x_k) - f\left(-\frac{f}{2}x_k^2 + (v_i)\, x_k \right) - E_i \right) (h^*)^2(x_k) + \frac{(hu)_i}{2} = 0. \tag{44}$$

Where x_k is any of the points of interest in the stencil and E_i is the energy of the system which must be constant for the stationary solution as well as $(hu)_i$ and v_i. In particular, this set of equations must be satisfied for all points in the centre cell C_i. Using the

known cell averages at C_i, (42) determines the values of $(hu)^*$ all over the stencil. From (40) we can compute the value of v_i knowing the cell average $(hv)_i$:

$$(hv)_i = \int_{x_{i-1/2}}^{x_{i+1/2}} h^*(x)v^*(x)dx = \int_{x_{i-1/2}}^{x_{i+1/2}} h^*(x)(-fx+v_i)dx \approx \sum_{p=1}^{n} \alpha_p \left(h(x_i^p)v_i - f\,h(x_i^p)x_i^p\right),$$

which means that

$$v_i = \frac{(hv)_i + f\sum_{p=1}^{n}\alpha_p h^*(x_i^p)x_i^p}{\sum_{p=1}^{n}\alpha_p h^*(x_i^p)}. \tag{45}$$

It remains to be computed the values of the stationary water depth $h^*(x_i^p)$. Substituting (45) in (44) we obtain that $h^*(x_i^p)$ must be a root of

$$g_p(x_i^1,\dots,x_i^n,E_i) = \left(gz(x_i^p) - f\left(-\frac{f}{2}\left(x_i^p\right)^2 + \left(\frac{(hv)_i + f\sum_{p=1}^{n}\alpha_p h^*(x_i^p)x_i^p}{\sum_{p=1}^{n}\alpha_p h^*(x_i^p)}\right)x_i^p\right) - E_i\right)(h^*)^2(x_i^p) + g(h^*)^3(x_i^p) + \frac{(hu)_i}{2}.$$

So, we have a system of non-linear equations $g_p = 0$ for $p = 1,\dots,n$ with $n+1$ variables $x_i^1,\dots,x_i^p,E_i$. To complete the system of equations, we have to add the following condition:

$$g_0(x_i^1,\dots,x_i^n,E_i) = \sum_{p=1}^{n}\alpha_p h^*(x_i^p) - h_i,$$

where $g_0 = 0$ means that the cell average is preserved by $h^*(x)$ at the cell C_i. Then, if we solve this non-linear system of equations, we know all point values at the cell C_i of the stationary water depth $h^*(x)$ and the local energy. With this data, we can now calculate v_i with (45) and with this value, we know $v^*(x)$ in the stencil. Also, as we know the energy E_i and v_i in the whole stencil, we can calculate $h^*(x)$ in the rest of the points of interest by solving the cubic equation (44).

This procedure, allows us to determine the values of the stationary solutions h^*, hu^* and hv^* in all the stencils for a general CWENO reconstruction procedure. These values are enough information to obtain an exactly well-balanced scheme for the shallow-water equations with Coriolis source terms according to the method described in section 2.

A.1. Particular case: third-order CWENO

We are going to give a complete example of this procedure for the **third-order** CWENO reconstruction. In this particular case, we perform the following steps:

1. We know that

$$v^*(x) = -fx + v_0,$$
$$\frac{1}{|I_i|}\int_{x_{i-1/2}}^{x_{i+1/2}} v^*(x)dx = v_i.$$

Since we cannot calculate v_i, we consider computing

$$(hv)_i = \int_{x_{i-1/2}}^{x_{i+1/2}} h^*(x)v^*(x)dx = 0.5v_0(h_0+h_1) + 0.5(-fx_0h_0 - fx_1h_1),$$

obtaining

$$v_0 = \frac{2(hv)_i + fx_0h_0 + fx_1h_1}{h_0+h_1},$$

knowing this expression, we can compute the potential

$$V(x) = -0.5fx^2 + x\frac{2(hv)_i + fx_0h_0 + fx_1h_1}{h_0+h_1}.$$

2. Considering the expression of the potential, we can set up a system of three equations

$$g_0(h_0,h_1,E) = 0.5(h_0+h_1) - h_i,$$

$$g_1(h_0,h_1,E) = gh_0^3 + \left(gz(x_0) - f\left(-0.5 f x_0^2 + x_0 \frac{2(hv)_i + f x_0 h_0 + f x_1 h_1}{h_0 + h_1} \right) - E_i \right) h_0^2 + \frac{(hu)_i}{2},$$

$$g_2(h_0,h_1,E) = gh_1^3 + \left(gz(x_1) - f\left(-0.5 f x_1^2 + x_1 \frac{2(hv)_i + f x_0 h_0 + f x_1 h_1}{h_0 + h_1} \right) - E_i \right) h_1^2 + \frac{(hu)_i}{2},$$

where $h_0 = h^*(x_0)$ and $h_1 = h^*(x_1)$. With these equations, we again have a system of three equations to be solved using Newton's method. We will initialize the variables with the cell average values.

3. Once the solutions have been calculated using Newton's method, we will have the values at the quadrature points h_1^*, h_2^*, the constant value hu^*, the energy E_i and the value v_0^* with which the solution stationary v^* is completely determined as well as the potential V. In this way, the rest of the point values of the solution are calculated with (42)-(44).

References

[1] M. Asunción, M. Castro, E. Fernández-Nieto, J. Mantas, S. Ortega, J. González Vida, Efficient gpu implementation of a two waves tvd-waf method for the two-dimensional one layer shallow water system on structured meshes, Comput. Fluids 80 (2013) 441–452.

[2] E. Audusse, F. Bouchut, M.-O. Bristeau, R. Klein, B. Perthame, A fast and stable well-balanced scheme with hydrostatic reconstruction for shallow water flows, SIAM J. Sci. Comput. 25 (6) (2004) 2050–2065.

[3] E. Audusse, R. Klein, D.D. Nguyen, S. Vater, Preservation of the discrete geostrophic equilibrium in shallow water flows, in: J. Fořt, J. Fürst, J. Halama, R. Herbin, F. Hubert (Eds.), Finite Volumes for Complex Applications VI Problems & Perspectives, Berlin, Heidelberg. Springer Berlin Heidelberg, 2011, pp. 59–67.

[4] J.P. Berberich, P. Chandrashekar, C. Klingenberg, High order well-balanced finite volume methods for multi-dimensional systems of hyperbolic balance laws, Comput. Fluids 219 (2021) 104858.

[5] A. Bermúdez, M.E. Vázquez, Upwind methods for hyperbolic conservation laws with source terms, Comput. Fluids 23 (8) (1994) 1049–1071.

[6] A. Bermúdez, X. López, M.E. Vázquez-Cendón, Finite volume methods for multi-component euler equations with source terms, in: Ninth International Conference on Computational Fluid Dynamics (ICCFD9), in: Computers & Fluids, vol. 156, 2017, pp. 113–134.

[7] F. Bouchut, Non-linear Stability of Finite Volume Methods for Hyperbolic Conservation Laws and Well-Balanced Schemes for Sources, Frontiers in Mathematics, Birkhauser, 2004.

[8] F. Bouchut, T.M. de Luna, A subsonic-well-balanced reconstruction scheme for shallow water flows, SIAM J. Numer. Anal. 48 (5) (2010) 1733–1758.

[9] F. Bouchut, J.L. Sommer, V. Zeitlin, Frontal geostrophic adjustment and nonlinear wave phenomena in one-dimensional rotating shallow water. Part 2. High-resolution numerical simulations, J. Fluid Mech. 514 (2004) 35–63.

[10] P. Brufau, M.E. Vázquez-Cendón, P. García-Navarro, A numerical model for the flooding and drying of irregular domains, Int. J. Numer. Methods Fluids 39 (3) (2002) 247–275.

[11] A. Canestrelli, A. Siviglia, M. Dumbser, E.F. Toro, Well-balanced high-order centred schemes for non-conservative hyperbolic systems. Applications to shallow water equations with fixed and mobile bed, Adv. Water Resour. 32 (6) (2009) 834–844.

[12] M. Castro, J.M. Gallardo, J.A. López-García, C. Parés, Well-balanced high order extensions of godunov's method for semilinear balance laws, SIAM J. Numer. Anal. 46 (2) (2008) 1012–1039.

[13] M. Castro, J. López-García, C. Madroñal, High order exactly well-balanced numerical methods for shallow water systems, J. Comput. Phys. 246 (2013) 242–264.

[14] M. Castro, C. Parés, Well-balanced high-order finite volume methods for systems of balance laws, J. Sci. Comput. 82 (48) (2020) 939–973.

[15] M.J. Castro, T.M. de Luna, C. Parés, Well-balanced schemes and path-conservative numerical methods, Handb. Numer. Anal. 18 (2017) 131–175.

[16] M.J. Castro, J.A. López, C. Parés, Finite volume simulation of the geostrophic adjustment in a rotating shallow-water system, SIAM J. Sci. Comput. 31 (1) (2008) 444–477.

[17] M.J. Castro, A.P. Milanés, C. Parés, Well-balanced numerical schemes based on a generalized hydrostatic reconstruction technique, Math. Models Methods Appl. Sci. 17 (12) (2007) 2055–2113.

[18] M.J. Castro Díaz, T. Chacón Rebollo, E.D. Fernández-Nieto, C. Parés, On well-balanced finite volume methods for nonconservative nonhomogeneous hyperbolic systems, SIAM J. Sci. Comput. 29 (3) (2007) 1093–1126.

[19] M.J. Castro Díaz, C. Chalons, T.M. de Luna, A fully well-balanced lagrange–projection-type scheme for the shallow-water equations, SIAM J. Numer. Anal. 56 (5) (2018) 3071–3098.

[20] T. Chacón Rebollo, A. Domínguez Delgado, E.D. Fernández Nieto, A family of stable numerical solvers for the shallow water equations with source terms, Comput. Methods Appl. Mech. Eng. 192 (1) (2003) 203–225.

[21] T. Chacón Rebollo, A. Domínguez Delgado, E.D.F. Nieto, Asymptotically balanced schemes for non-homogeneous hyperbolic systems – application to the shallow water equations, C. R. Math. 338 (1) (2004) 85–90.

[22] P. Chandrashekar, C. Klingenberg, A second order well-balanced finite volume scheme for euler equations with gravity, SIAM J. Sci. Comput. 37 (3) (2015) B382–B402.

[23] A. Chertock, M. Dudzinski, A. Kurganov, M. Lukáčová-Medvid'ová, Well-balanced schemes for the shallow water equations with coriolis forces, Numer. Math. 138 (2018) 939–973.

[24] I. Cravero, G. Puppo, M. Semplice, G. Visconti, Cweno: uniformly accurate reconstructions for balance laws, Math. Comput. 87 (312) (2018) 1689–1719.

[25] D. Levy, G. Puppo, G. R, Central weno schemes for hyperbolic systems of conservation laws, M2AN 33 (3) (1999) 547–571.

[26] V. Desveaux, A. Masset, A fully well-balanced scheme for shallow water equations with Coriolis force, Commun. Math. Sci. 20 (7) (2022) 1875–1900.

[27] E.D. Fernández-Nieto, D. Bresch, J. Monnier, A consistent intermediate wave speed for a well-balanced hllc solver, C. R. Math. 346 (13) (2008) 795–800.

[28] E. Gaburro, M.J. Castro, M. Dumbser, Well-balanced arbitrary-Lagrangian-Eulerian finite volume schemes on moving nonconforming meshes for the Euler equations of gas dynamics with gravity, Mon. Not. R. Astron. Soc. 477 (2) (2018) 2251–2275.

[29] I. Gómez-Bueno, M.J. Castro, C. Parés, G. Russo, Collocation methods for high-order well-balanced methods for systems of balance laws, Mathematics 9 (15) (2021).

[30] S. Gottlieb, On high order strong stability preserving runge-kutta and multi step time discretizations, J. Sci. Comput. 25 (2005) 105–128.

[31] I. Gómez-Bueno, M.J. Castro, C. Parés, High-order well-balanced methods for systems of balance laws: a control-based approach, Appl. Math. Comput. 394 (2021) 125820.

[32] A. Harten, P.D. Lax, B. van Leer, On Upstream Differencing and Godunov-Type Schemes for Hyperbolic Conservation Laws, Springer, Berlin Heidelberg, Berlin, Heidelberg, 1997, pp. 53–79.

[33] C. Klingenberg, G. Puppo, M. Semplice, Arbitrary order finite volume well-balanced schemes for the euler equations with gravity, SIAM J. Sci. Comput. 41 (2) (2019) A695–A721.
[34] C. Sánchez-Linares, T. Morales de Luna, M. Castro Díaz, A hllc scheme for ripa model, Appl. Math. Comput. 272 (2016) 369–384.
[35] E.F. Toro, The weighted average flux method applied to the euler equations, Ser. A, Phys. Eng. Sci. 341 (1992) 499–530.
[36] E.F. Toro, Riemann Solvers and Numerical Methods for Fluid Dynamics, Springer, Berlin, Heidelberg, 2009.
[37] E.F. Toro, The hllc riemann solver, Shock Waves 29 (2019) 1065–1082.
[38] M. Tort, T. Dubos, F. Bouchut, V. Zeitlin, Consistent shallow-water equations on the rotating sphere with complete coriolis force and topography, J. Fluid Mech. 748 (2014) 789–821.
[39] V. González-Tabernero M. J. C, J.A. García-Rodríguez, High-order well-balanced finite volume schemes for 1d and 2d shallow-water equations with coriolis forces, in: Proceedings HYP 2022, (to appear).
[40] B. van Leer, Towards the ultimate conservative difference scheme. V. A second-order sequel to godunov's method, J. Comput. Phys. 32 (1979) 101–136.
[41] Y. Xing, C.-W. Shu, High order finite difference weno schemes with the exact conservation property for the shallow water equations, J. Comput. Phys. 208 (1) (2005) 206–227.
[42] X. Zhang, C.-W. Shu, On maximum-principle-satisfying high order schemes for scalar conservation laws, J. Comput. Phys. 229 (2010) 3091–3120.